Essential Role of Couplings between Hearing Nonlinearities

A. Kern and R. Stoop

Institute of Neuroinformatics, University/ETH of Zürich, Winterthurerstrasse 190, 8057 Zürich, Switzerland
(Received 4 February 2003; published 19 September 2003)

Hopf-type nonlinearities have been recently found to be the basic mechanism of the mammalian cochlear response. Physiology requires that these nonlinearities be coupled. By suitably implementing a biomorphic coupling scheme of cochlear nonlinearities, we obtain a simple cochlea model that faithfully reproduces measured basilar membrane response, validating the utility of the Hopf amplifier concept. Our results demonstrate that the correct coupling between nonlinearities is as important as the nonlinearities themselves.

An outstanding open problem in physics is to find a realistic model of the mammalian fluid-filled hearing organ, the cochlea. Cochlear modeling has a long tradition, starting with Helmholtz in 1863, who revealed the tonotopic principle [1]. A second important milestone was von Békésy's discovery of traveling waves along the basilar membrane (BM) [2], which gave rise to passive hydrodynamic models [3]. Already in 1948 it was conjectured that an active amplification must be present in the cochlea [4]. The discovery of otoacoustic emissions [5] (the production of sounds by the ear itself) later provided evidence for this mechanism. Since then, various experiments revealed that the outer hair cells (OHC), which reside on top of the BM, are the source of active amplification. Recently, amphibian hair cells (that are the ancestors of mammalian OHC) were shown to display Hopf-type response [6]. In fact, there are recent proposals [7,8] of considering Hopf bifurcators as the basic elements for auditory modeling, since they correctly capture the basic phenomena of hearing: compression of the dynamic range, sharper tuning for lower intensity sounds, and the generation of combination tones. However, the basic model put forward in [7] matches poorly with realistic cochlear responses. In this Letter, we show that in order to obtain a realistic BM response, as measured, e.g., by Ruggero [9] [see Figs. 4(a) and 4(b)], one needs to extend the fundamental model by biomorphic, physiologically motivated couplings. This biomorphic nature of our approach is the basic difference to a concurrent approach recently published by Magnasco [10].

The Hopf bifurcator.—We start by providing a summary of the approach proposed in [7]. The fundamental ingredient of the Hopf cochlea is the Hopf differential equation

$$\dot{z} = (\mu + i\omega_0)z - |z|^2 z + Fe^{i\omega t}, \qquad z(t) \in \mathbb{C}, \quad (1)$$

where ω_0 is the natural frequency of the oscillation, $\mu \in \mathbb{R}$ denotes the bifurcation parameter, and $F(t) = Fe^{i\omega t}$ is an external periodic forcing with frequency ω. In the absence of external forcing, (1) describes the generic differential equation displaying a Hopf bifurcation [11]: For $\mu < 0$, the solution $z(t) = 0$ is a stable

fixed point, whereas for $\mu > 0$, the fixed-point solution becomes unstable and a stable limit cycle of the form $z(t) = \sqrt{\mu}e^{i\omega_0 t}$ appears.

For an input $F(t)$, $z(t)$ can be considered as the amplified signal. The steady-state solution for periodic forcings is obtained by the ansatz $z(t) = Re^{i\omega t + i\phi}$, where a 1:1 locking between signal and system was assumed [12]. The response amplitude R is then determined from a cubic equation in R^2,

$$F^2 = R^6 - 2\mu R^4 + [\mu^2 + (\omega - \omega_0)^2]R^2. \quad (2)$$

For $\mu = 0$ and close to resonance $\omega = \omega_0$, the response $R = F^{1/3}$ emerges, which forces the gain $G = R/F = F^{-2/3}$ to increase towards infinity as F approaches zero. This implies a compressive nonlinearity, for any stimulus size. For $\mu < 0$, maintaining $\omega = \omega_0$, we obtain the response $R = -F/\mu$ for weak stimuli F. As F increases, the term R^6 in (2) can no longer be neglected, and, as $R^6 \approx \mu^2 R^2$, the compressive nonlinear regime is entered. The transition point occurs at $F_{cnl} \approx (-\mu)^{3/2}$. Therefore, the response R is nearly linear for weak stimuli F, while for moderate stimuli the differential gain of the system, dR/dF, decreases with increasing stimulus intensity. Away from the resonance, the last term in (2) dominates. In this case, the response is linear for every input, as $R \approx F/(\omega - \omega_0)$. For $\mu > 0$, stable limit cycles emerge.

Dispersion relation and first tonotopic map.—Here, the passive behavior of the cochlear fluid is shown to follow from basic hydrodynamics. The Hopf amplifiers in the cochlea are mechanically connected to the BM. Mediated by the cochlear fluid, incoming sound pressure variations transform into a hydrodynamic traveling wave along the BM [2,13]. The fluid can be considered incompressible and inviscid [13]. As the BM displacements are small (of the order of 10^{-8} m), a linear theory of the passive components is appropriate. This assumption is well supported by experimental observations: (i) nonlinearities disappear postmortem [14], (ii) active amplification is disabled by appropriate drugs [15], (iii) linear BM input-output functions are observed for intense sound levels [16], at which active amplification is not effective. This suggests that the source of cochlear nonlinearity is in the active

processes. Because of the linearity, the membrane-fluid behavior can be described by a water surface wave [17,18], endowed with a surface mass density m and exponentially decreasing transversal stiffness

$$E(x) = E_0 e^{-\alpha x}. \qquad (3)$$

The surface wave is characterized by a dispersion relation that can be derived from linearizing the boundary conditions $p_{BM} = -\rho \frac{\partial \phi}{\partial t}$ of the Laplace equation $\Delta \phi = 0$ [19,20] (where ρ is the fluid density). The pressure exerted by the surface has the form $p_{BM} = E\zeta + m\ddot{\zeta}$, where $\zeta(x, t)$ denotes the deviation of the free surface from equilibrium. This entrains [18] the dispersion relation

$$k(x, \omega) \tanh[k(x, \omega)h] = \rho \omega^2 / [E(x) - m\omega^2], \qquad (4)$$

where h denotes the water depth and $k = 2\pi/\lambda$ the wave number. The characteristic frequency of (4),

$$\omega_c(x) = \sqrt{E(x)/m}, \qquad (5)$$

provides an explicit relation between BM location $x = x_c(\omega)$ and frequency $\omega = \omega_c(x)$, called the "first tonotopic map." Equation (4) shows that $k(x, \omega)$ diverges, as ω approaches $\omega_c(x)$.

The stationary energy density distribution along the cochlear duct, denoted by $e(x, \omega)$, is a key quantity in our approach. For its determination, the dependence of the group velocity, $v(x, \omega)$ on $\{x, \omega\}$, will be needed. From (4), we obtain

$$v = \frac{\partial \omega}{\partial k} = \frac{E(x)\rho}{2\omega} \frac{kh + \sinh(kh)\cosh(kh)}{[mk\sinh(kh) + \rho\cosh(kh)]^2}. \qquad (6)$$

Let ω be fixed. As x approaches $x_c(\omega)$, $k \to \infty$ and $\sinh(kh), \cosh(kh) \sim \exp(kh)$, which implies that $v \to 0$: The traveling wave stalls at the point of (passive) resonance. As a consequence, energy density and wave amplitude diverge if no dissipation is included in the model. In the presence of (arbitrarily small) attenuating effects, dissipative losses will be accumulated over many wave cycles as $x_c(\omega)$ is approached. The wave amplitude will therefore reach a maximum at $x < x_c(\omega)$, which is consistent with von Békésy's original observations of the passive cochlear behavior [2].

Cochlear differential equation.—The central modeling step is how to couple the Hopf amplifiers to the passive traveling wave. For propagating (linear and nonlinear) waves, for $e(x, \omega)$ the energy balance equation

$$\partial e/\partial t + \partial (ve)/\partial x = 0 \qquad (7)$$

applies [19]. For obtaining the steady-state distribution of the one-dimensional energy density $e(x, \omega)$, we use the ansatz $\frac{\partial e}{\partial t} =: -a + de$, which incorporates the two antagonistic contributions by the internal viscous losses $(d(x, \omega) = 4(\mu/\rho)[k(x, \omega)]^2$, where μ is the viscosity [20]), vs the local energy supply by the active Hopf amplification, $a(\cdot)$. From this, we immediately arrive at our fundamental cochlea differential equation

$$\frac{\partial e(x, \omega)}{\partial x} = -\frac{e(x, \omega)}{v(x, \omega)}\left[\frac{\partial v(x, \omega)}{\partial x} + d(x, \omega)\right]$$
$$+ \frac{a[x, e(x, \omega), \omega]}{v(x, \omega)}, \qquad (8)$$

where the specific form of $a(\cdot)$ still remains to be derived.

Second tonotopic map.—The active amplification is based upon an array of Hopf-type power sources with varying natural frequencies $\omega_0(x)$, arranged along the BM (Fig. 1). For a given forcing frequency ω, the Hopf amplifiers at locations x satisfying $\omega_0(x) \approx \omega$ are maximally excited, which induces a second tonotopic map [21]. For intermediate and large frequencies ($\omega/2\pi > 1000$ Hz), we propose the relation [22]

$$\omega_0(x) = \omega_c(x)e^{-(\alpha/2)\Delta x}, \qquad (9)$$

where Δx is independent of x. As can be deduced from Eqs. (3) and (5), the location of maximum excitation is given by $x_0(\omega) = x_c(\omega) - \Delta x$. This expression is in accordance with the requirement that the amplification of the traveling wave must occur before $x_c(\omega)$ is reached, where viscous losses lead to a precipitous decay of wave amplitude. The frequency selectivity at different locations on the BM can be expressed as the relative bandwidth $\Delta\omega/\omega$ [$\Delta\omega = \omega_c - \omega_0$; see Fig. 2(a)] of the frequency response. Expression (9) guarantees that the frequency selectivity remains constant for low sound levels [see Fig. 4(a)], which agrees with the fact that psychoacoustical auditory filter bandwidths increase linearly in ω for $\omega/2\pi > 1000$ Hz [24,25].

Derivation of $a(x, e, \omega)$.—The explicit relation between $a(x, e, \omega)$ and R follows from the biophysics of cochlear hair bundles. The deflection of the OHC hair bundle starts the active force generation, by motility of the soma or by active stereocilia motion. As a consequence, the stereocilia tip links, which are tethered to ion transduction channels, induce tensile forces on the latter, which leads to changes in the channel conformation. In mammals, the ensuing membrane potential change modifies the length of the cell soma (electromotility
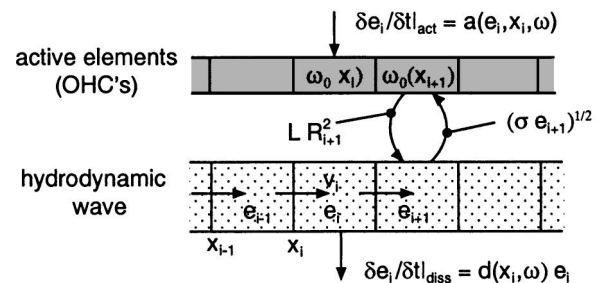
FIG. 1. Discretized Hopf cochlea model [Eq. (8)]. The hydrodynamic traveling wave energy propagates with velocity $v_i = v(x_i, \omega)$. In addition to the ensuing convective change [Eq. (7)], the energy density $e_i = e(x_i, \omega)$ is augmented by the action of the active amplifiers [Eqs. (11) and (2)], with natural frequencies $\omega_0(x_i)$ [Eq. (9)].
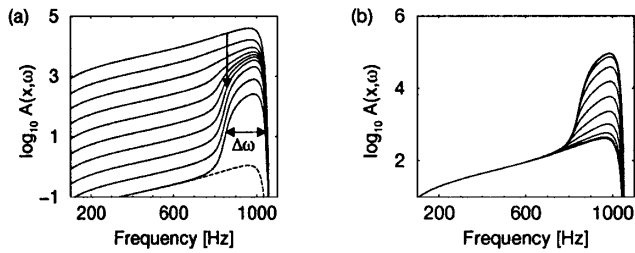
FIG. 2. Modeled local BM response from an array of Hopf bifurcators, no coupling [based on Eq. (8)]. (a) BM frequency response at $x_c(\omega/2\pi = 1000$ Hz); dashed line: frequency response of the passive model. (b) BM gain, relative to stapes motion [23].

[26]) and induces an active force on the BM. For lower vertebrates, the active mechanism may directly proceed via transduction channel dynamics (active hair bundle motility [6]).

For both cases, we can regard the tensile forces $F(t)$ as the input to the Hopf system (1) [6,26]. By Hooke's law, $F(t)$ is proportional to the hair bundle displacement, which in turn is proportional to the BM amplitude $A(x, \omega)$. Kinetic and potential energy, averaged over one cycle, contribute equally to the total energy. When combined with $e_{pot}(x, \omega) = \frac{1}{4}E(x)A(x, \omega)^2$, this leads to

$$A(x, \omega) = [2e(x, \omega)/E(x)]^{1/2}. \tag{10}$$

For fixed position x, the force amplitude is thus given by $F = \sqrt{\sigma e}$, where σ can be seen as the transfer parameter from A to F. The ensemble of Hopf oscillators active at location x then delivers a force, whose amplitude will be proportional to R [Eq. (2)]. This leads to a BM displacement proportional to the square root of the energy supplied by the active process. Expressing the associated proportionality constant by L, we obtain

$$a(e, x, \omega) = L\{R[\sqrt{\sigma e(x, \omega)}]\}^2, \tag{11}$$

with the characteristic frequency of the Hopf oscillators being determined by the second tonotopic map (9). Equations (3), (6), (8), (11), and (10) provide the connection between our cochlea model and physiological measurements.

Simulations.—To tune our general approach to experimental results from mammalian cochleae, we observe that the sharp spatial tuning of R in the Hopf system suggests that one regard σ and L as constant over the spatial support of the oscillator array, for each ω. μ is chosen in order to match the amplification slope observed for low intensities [slope left to the response peak; see the vertical arrow in Fig. 2(a)]. From Eq. (2) it can be concluded [22] that the transition point between the linear and the compressive regime is determined by σ only, which helps to select an appropriate value of σ. For σ fixed, the gain $a(x, e, \omega)/e$ is determined by L, see Eq. (11), so that also this parameter can be set appropriately [27]. The presented simulation results then emerge

from inserting these parameters into Eqs. (3), (6), (8), and (11) or (12), according to the degree of sophistication. Equation (10) then allows for the comparison with experimental data.

In contrast to Ref. [7], in [8] it was argued that μ should be considered critically self-tuned at the bifurcation. This indeed would be favorable for the explanation of otoacoustic emissions and increase the sensitivity to newly arriving stimuli. As can be seen from a recent implementation of this approach (see [10]), it does not, however, explain the cochlear response for sustained stimulation. The obtained response is nonlinear for arbitrarily low stimuli, and a rampant response occurs at x_0. Both effects are not supported by measurements (where the first observation was already anticipated by [7]). Therefore, the choice of $\mu < 0$ seems more natural. A value of $\mu \approx -200$ leads to a spatial bandwidth of the oscillator that is in excellent agreement with physiological measurements [22].

Results.—The inclusion of Hopf amplifiers according to Eqs. (3), (6), (8), and (11) leads to results that already very well reproduce the main features of the cochlear response [see Fig. 2(a)]. Only upon a close inspection, remaining discrepancies to measurements emerge: Experimental curves display a response peak shift towards lower frequencies with increased stimulus intensities and an associated increase in response bandwidth [Fig. 4(a)] that are not optimally reproduced. Inclusion of the most basic biomorphic couplings is able to remedy these shortcomings to a large extent.

Refinements.—The picture of a vibrating BM loaded with an array of Hopf oscillators suggests taking two couplings into account. Apart from the obvious direct coupling among Hopf-type oscillators (by means of physical connections provided by the Deiters cells [28]), a coupling is provided by the BM itself. When distorted from its equilibrium position by an amount of $\zeta(x)$, the BM generates by means of the surface tension $T(x)$ a restoring force $F_s = T(x)\frac{\partial^2 \zeta(x)}{\partial x^2}$ [20]. F_s modifies the dispersion relation (4) by replacing $E(x)$ with $E(x) + k(x, \omega)^2 T(x)$, which leads to a modified ν in the cochlea equation (8). Apart from this, the simulations proceed as described earlier. The inclusion of this coupling leads to a significant improvement of the results [see Fig. 3(a), where $T(x) = 10^{-5}E(x)$ has been used [29]].
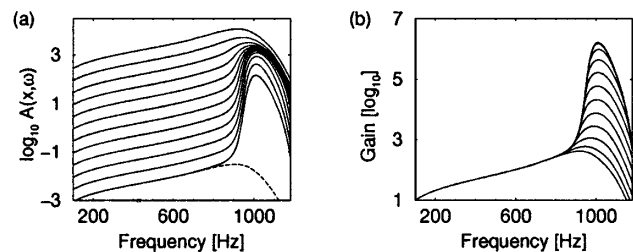
FIG. 3. BM response of the Hopf amplication model with surface tension. (a) Frequency response; (b) gain.
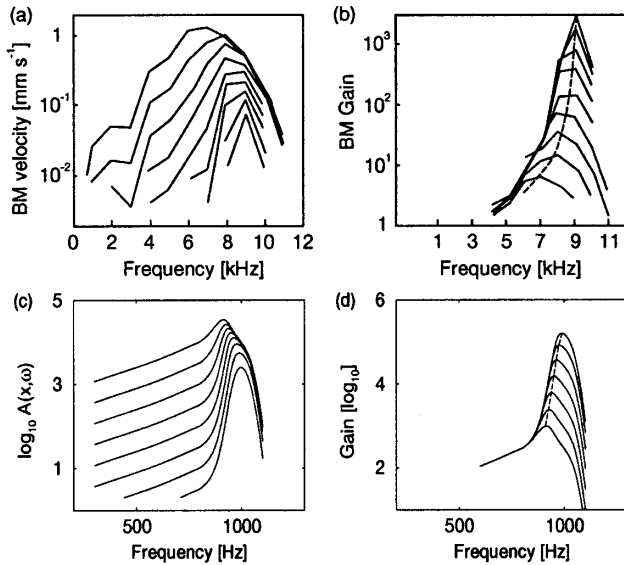
FIG. 4. Experimental BM frequency response (a) and gain (b), adapted from [9]. Frequency response (c) and gain (d) from the Hopf amplification model with surface tension and feedforward coupling.

The inclusion of the above-mentioned direct coupling is of secondary importance and will only be sketched. We implemented this feedforward coupling as the substrate of a second energy propagation mode that in the vicinity of the active resonance location is powered by the energy density $e(x, \omega)$. We restrict the feedforward integration to a range Δx, over which we use a constant weight. The amplification $a_2(x, e, \omega)$ of the energy density $e_2(x, \omega)$ of the second mode then amounts to

$$\frac{1}{\Delta x} \int_{x-\Delta x}^{x} (R\{\sqrt{\sigma_{cp}(\omega)[e(x', \omega) + M e_2(x', \omega)]}\})^2 dx',$$

where $\sigma_{cp}(\omega)$ is the associated scaling parameter and $M > 0$ is the feedforward coupling strength. This relation, together with the energy balance in the steady-state situation [similar to Eq. (7)], allows the determination of $e_2(x, \omega)$. The cochlear amplification $a(x, e, \omega)$, when embracing $e_2(x, \omega)$, assumes the form

$$a(\cdot) = L(\omega)(R\{\sqrt{\sigma_{cp}(\omega)[e(x, \omega) + N e_2(x, \omega)]}\})^2, \quad (12)$$

where the additional term under the square root originates from the feedforward coupling and N denotes the coupling strength from the second to the first mode.

Inserting Eq. (12) instead of (11) into the cochlea equation (8) leads to results yet closer to the measured cochlear response (see Fig. 4), illustrating, how coupling schemes are important for modeling the correct cochlear response behavior. As coupling generically favors coherent in-phase oscillations [30], coupling also may account for the emergence of spontaneous otoacoustic emissions. Note the generality of our approach: Further couplings can be included analogously to the above, by defining additional modes of energy propagation that will lead to further modifications of the term $a(\cdot)$.

[1] H. Helmholtz, *Die Lehre von den Tonempfindungen als Physiologische Grundlage für die Theorie der Musik* (Vieweg, Braunschweig, 1863).
[2] G. von Békésy, *Experiments in Hearing* (McGraw-Hill, New York, 1960).
[3] E. De Boer, in *The Cochlea*, edited by P. Dallos, A. Popper, and R. Fay, Springer Handbook of Auditory Research (Springer, New York, 1996), pp. 258–317.
[4] T. Gold, Proc. R. Soc. London B **135**, 492 (1948).
[5] D. Kemp, J. Acoust. Soc. Am. **64**, 1386 (1978).
[6] P. Martin and A. Hudspeth, Proc. Natl. Acad. Sci. U.S.A. **98**, 14 386 (2001).
[7] V. Eguíluz, M. Ospeck, Y. Choe, A. Hudspeth, and M. Magnasco, Phys. Rev. Lett. **84**, 5232 (2000).
[8] S. Camalet, T. Duke, F. Jülicher, and J. Prost, Proc. Natl. Acad. Sci. U.S.A. **97**, 3183 (2000).
[9] M. Ruggero, Curr. Opin. Neurobiol. **2**, 449 (1992).
[10] M. Magnasco, Phys. Rev. Lett. **90**, 058101 (2003).
[11] E. Hopf, Ber. Math.-Phys., Sächs. Akad. d. Wiss. Leipzig **94**, 1 (1942).
[12] Higher harmonics are not generated at moderate intensities, where the pronounced nonlinear behavior of the cochlea emerges.
[13] E. De Boer, Phys. Rep. **62**, 87 (1980).
[14] W. Rhode, in *Basic Mechanisms in Hearing*, edited by A. Møller (Academic Press, Orlando, 1973), pp. 49–63.
[15] C. Wier, E. Pasanen, and D. McFadden, J. Acoust. Soc. Am. **84**, 230 (1988).
[16] P. Sellick, R. Patuzzi, and B. Johnstone, J. Acoust. Soc. Am. **72**, 227 (1982).
[17] B. Peterson and L. Bogert, J. Acoust. Soc. Am. **22**, 369 (1950).
[18] R. Patuzzi, in *The Cochlea* (Ref. [3]), pp. 187–257.
[19] G. Whitham, *Linear and Nonlinear Waves*, Pure and Applied Mathematics (Interscience Publishers, New York, 1999).
[20] J. Lighthill, *Waves in Fluids* (Cambridge University Press, Cambridge, 2002), 2nd ed.
[21] A second tonotopic map was first proposed in J. Allen and P. Fahey, J. Acoust. Soc. Am. **94**, 809 (1993).
[22] A Kern, Ph.D. thesis, Swiss Federal Institute of Technology (ETH), Zürich, 2003.
[23] Parameters are $\sigma = 19.3$, $L = 0.75$ (active model without additional coupling).
[24] B. Glasberg and B. Moore, Hear. Res. **47**, 103 (1990).
[25] B. Moore, in *Hearing*, edited by B. Moore (Academic Press, London, 1995), Chap. 5, pp. 161–205.
[26] M. Ospeck, X.-X. Dong, and K. Iwasa, Biophys. J. **84**, 739 (2003).
[27] It can be shown that for the whole frequency range $f > 1000$ Hz, σ and σL can be approximated by power functions in the stimulation frequency ω as $\sigma = \sigma_0(\omega/\omega_0)^2$ and $\sigma L = \sigma_0 L_0(\omega/\omega_0)^3$, where σ_0 and ω_0 are reference quantities [22].
[28] C. Geisler and C. Sang, Hear. Res. **86**, 132 (1995).
[29] This leads to $T = 0.02$ N m^{-1} at resonance.
[30] R. Stoop, K. Schindler, and L. Bunimovich, Neurosci. Res. **36**, 81 (2000).